Hindawi
International Transactions on Electrical Energy Systems
Volume 2023, Article ID 9828746, 1 page
https://doi.org/10.1155/2023/9828746

Retraction

Retracted: Optical Fiber Multiparameter Detection and Numerical Simulation and Characteristics of Water Quality Particulate Matter Based on Single-Photon Detection Technology

International Transactions on Electrical Energy Systems

Received 28 November 2023; Accepted 28 November 2023; Published 29 November 2023

This article has been retracted by Hindawi, as publisher, following an investigation undertaken by the publisher [1]. This investigation has uncovered evidence of systematic manipulation of the publication and peer-review process. We cannot, therefore, vouch for the reliability or integrity of this article.

Please note that this notice is intended solely to alert readers that the peer-review process of this article has been compromised.

Wiley and Hindawi regret that the usual quality checks did not identify these issues before publication and have since put additional measures in place to safeguard research integrity.

We wish to credit our Research Integrity and Research Publishing teams and anonymous and named external researchers and research integrity experts for contributing to this investigation.

The corresponding author, as the representative of all authors, has been given the opportunity to register their agreement or disagreement to this retraction. We have kept a record of any response received.

References

[1] Q. Xu, C. Gao, and C. Zhou, "Optical Fiber Multiparameter Detection and Numerical Simulation and Characteristics of Water Quality Particulate Matter Based on Single-Photon Detection Technology," *International Transactions on Electrical Energy Systems*, vol. 2022, Article ID 3170082, 10 pages, 2022.

Hindawi
International Transactions on Electrical Energy Systems
Volume 2022, Article ID 3170082, 10 pages
https://doi.org/10.1155/2022/3170082

Research Article

Optical Fiber Multiparameter Detection and Numerical Simulation and Characteristics of Water Quality Particulate Matter Based on Single-Photon Detection Technology

Quan Xu,[1,2] **Cuiyun Gao**,[1,2] **and Chun Zhou**[1]

[1]*School of Electronic and Information Engineering, Anhui Jianzhu University, Hefei 230601, Anhui, China*
[2]*Power Quality Analysis and Load Detection Technology Laboratory, Anhui Jianzhu University, Hefei 230601, Anhui, China*

Correspondence should be addressed to Quan Xu; xuquan@ahjzu.edu.cn

Received 25 August 2022; Revised 15 September 2022; Accepted 22 September 2022; Published 10 October 2022

Academic Editor: Nagamalai Vasimalai

Water quality testing is of great significance for daily water use or water use in high precision manufacturing. The use of single-photon detection technology to detect water particles is one of the important methods of physical water quality detection. However, the current water quality particle detection technology needs to be improved in the range and accuracy of turbidity detection. The paper aims to use single-photon detection technology to design a fiber optic turbidity detection system to solve the current problems of small turbidity detection range and low accuracy in a large range. In response to this, this paper has made an in-depth understanding of single-photon detection technology and designed two sets of detection schemes using the performance of photons. The first set is the transmission optical fiber turbidity detection, which can effectively detect the ultralow turbidity range and a wide range of water quality particles. The second set is a scattering optical fiber turbidity detection system, which can effectively detect water particles in the low and medium turbidity range. In this paper, the two systems were integrated into a whole system, so the results of the two detection methods can also be compared, and the detected turbidity can be obtained more accurately. The experimental results showed that for the transmission optical fiber turbidity detection system, the detection effect of the system was the best under the incident light intensity of 11 wm, and the fitting value was 0.99; for the scattering optical fiber turbidity detection system, the detection effect of the system was the best under the incident light intensity of 4 wm, and the fitting value was 0.99.

1. Introduction

Water is one of the most precious resources that nature bestows on mankind. It is indispensable in life and plays an important role in agriculture, industry, and economic development. However, water is also a scarce resource for mankind. In areas with extreme water scarcity, even human survival is a problem, for example, China's water resources. China is a country with a mild water shortage. Due to China's large population, the distribution of water resources is uneven. With the Yangtze River as the boundary, the south has nearly 80% of freshwater resources. Therefore, more perfect measures must be taken for protecting water resources. In this regard, wastewater treatment is a major and sustainable way to protect water resources. It is a powerful measure for the efficient use of water resources to treat and reuse the sewage produced by humans. However, whether the treated sewage can meet the standard, whether it can be reused, and where it can be applied are all issues that need to be considered. The most important of these issues is water quality testing. By using single-photon technology to detect water quality particles, it is possible to judge the water quality and then detect whether the water quality meets the standard and whether it can be reused. Therefore, from this aspect, it is necessary to use single-photon technology to design a fiber optic turbidity detection system to detect water quality treatment.

Single-photon technology is widely used in ranging, turbidity detection, and other places. Many scholars have conducted research on single-photon technology. Passig detected single vessel plumes from distances of several kilometers by

single particle mass spectrometry. He analyzed the metal content of individual particles preserved during atmospheric transport, which led to a dramatic increase in the accuracy of detection [1]. Jia designed and fabricated silicon carbide microdisks and experimentally characterized their multimode resonances in air and water [2]. To effectively assess the health risks of cyanobacterial blooms, MD Graham devised an early warning system. The system was capable of rapidly detecting species of interest and determining whether their cellular concentrations exceeded the recommended guidelines [3]. Sultana proposed a new approach to rainwater harvesting. He first conducted multiparameter detection of water quality particulate matter and collected it after confirming that it was drinkable, which solved the drinking water problem in some water deficient areas [4]. Asbach studied the performance of the water-based personal condensation particle counter PUFP C100 when sampling a variety of different test aerosols [5]. Many scholars have conducted research on the application of single-photon technology in industry and biomedicine, and the research results have also been very satisfactory. However, their research only focused on the existing performance of single-photon technology and did not improve or develop new applications of single-photon technology.

For water quality testing, scholars have been carrying out research for a long time. Huffaker presented a new platform for stand-alone absorbing and multiplying photodiodes. Out of the 4400 nanowires that make up a photodiode, each event was confined to one nanowire, and the platform was used for single-photon detection [6]. Deng designed and developed a photodiode-based high dynamic range photodetection module, which simplifies system operation and can easily detect various incident light intensities [7]. To cope with the large error in light intensity measurement in extreme cases, Zhou improved the UV (ultraviolet) single-photon detection technology and designed a high performance UV photodiode with a diameter of 300 μm [8]. Silver demonstrated an upconversion-based multiplexing scheme for single-photon detection using a waveguide with multiple phase-matched peaks [9]. Ren combined dual-comb-based laser ranging technology with time-correlated single-photon counting technology to make single-photon measurements more precise. He also demonstrated its feasibility for precise laser ranging under photons [10]. However, their water quality detection methods are still stuck in the traditional light absorption law detection method, which has a small detection range and low precision.

The innovations of this paper are as follows: (1) the single-photon detection technology was improved so that the single-photon detection technology can be better applied to the detection of water particles. (2) An optical fiber turbidity detection system of the transmission type and scattering type was designed, which greatly improved the range and accuracy of turbidity detection.

2. Optical Fiber Water Quality Particle Detection

2.1. Optical Fiber Detection Technology. Optical fibers are often used as broadband transmission media in daily use. Due to the silica material of optical fibers, the light source can be totally reflected in the structure [11, 12]. Optical fiber now has a strong application in electronic technology. Since the transmission of light inside the fiber is total reflection, the transmission loss of the signal in the fiber is much lower than the loss in the conduction of the wire. Additionally, since the main raw material for optical fiber production is silicon, which is very abundant on Earth and easy to mine, the price is very cheap. All of these have prompted many optical fibers to be used in daily production and life. The schematic diagram of fiber structure and propagation is shown in Figure 1.

In 1977, optical fiber sensing technology was discovered and gradually began to be applied in various fields. With the rapid popularization of Internet construction, optical fiber communication technology has developed rapidly [13, 14]. Optical fiber sensing technology has also developed various properties, such as temperature, humidity, speed, sound field, and magnetic field. Optical fiber as a medium can pass light waves with ultralow loss. Optical fiber sensing technology transmits external signals in the form of light waves through optical fibers [15, 16]. Since the transmission of light waves in the optical fiber is less affected by the outside world, optical fiber sensing technology is a relatively stable sensing technology. The emergence of optical fiber sensors has enabled many water quality detection equipment to develop toward strong adaptability, compactness, portability, and intelligence. The physical map of optical fiber and optical cable is shown in Figure 2.

2.2. Principle of Detection of Particulate Matter in Water Quality

2.2.1. Lambert –Beer Transmission Law. Transmission and reflection occur when a wave propagates from one medium to a different medium and when there are discontinuities in the medium through which the wave propagates. In optics, there are many materials to which Lambert Beer's law of transmission can be applied. It is suitable for all electromagnetic radiation and light-absorbing material measurements, including gases, liquids, and solids, and even the microscopic world of molecules, atoms, and ions. The use of the transmission law can shine brightly in quantitative measurements. The basic principle of using the Lambert–Beer transmission law is to test water quality particulate matter and to use the degree of light loss to judge the abundance of water quality particulate matter. When the photons are emitted from a light source, in the turbid water, some particles would reflect, refract, and absorb the irradiated light, which causes the light to be hindered in the process of propagation. As long as the direction of light propagation and the intensity of light are well controlled, and when the change characteristics of the weakening of light energy are detected and numerically simulated, the particle concentration of water quality can be obtained [17, 18].

Light travels through the medium. Since the medium has certain obstacles to the transmission of light, the output light

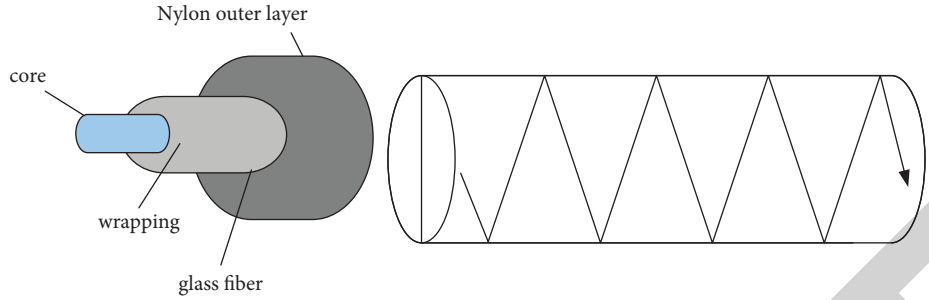

Figure 1: Optical fiber structure and transmission mode.

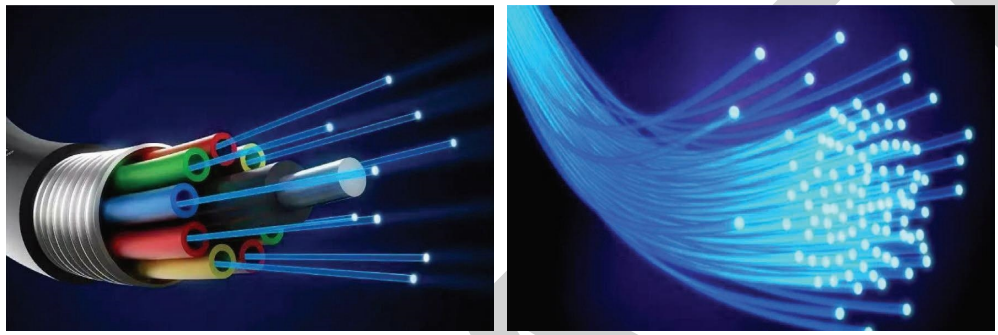

fiber optic cable optical fiber

Figure 2: Optical cable and optical fiber.

would have a certain loss. According to the Lambert–Beer transmission law, the farther the light travels, the greater the loss of light [19, 20]. It is assumed that the medium in Figure 3 is uniform, and then, this process can be expressed by the following formulas.

$$d_I = \alpha I d_x, \tag{1}$$

$$\int_{I_o}^{I_t} \frac{d_I}{I} = \int_0^l \alpha d_x, \tag{2}$$

$$I_t = I_o e^{\alpha l}. \tag{3}$$

Among them, l is the distance of light penetration; I_o, I_t are the intensity of the incident light and outgoing light, respectively; d_I, d_x are the loss of light and the dielectric layer. The incident light I_o causes loss after passing through the dielectric layer d_x. The fact that α must be negative can be obtained by using the knowledge of integration as shown in formula (2).

It can be seen that the above formulas are aimed at a solid substance with a homogeneous medium. The internal structure of solid matter is relatively stable, and the attenuation of light is proportional to the transmission distance and would not be affected by other factors [21]. However, if the solid is replaced by a liquid substance, the above formulas cannot directly denote the attenuation coefficient of light. This is due to the fact that in liquid substances, molecular motion is more active, and the propagation of photons cannot be well controlled [22]. Therefore, the weakening process of light is not only related to the distance

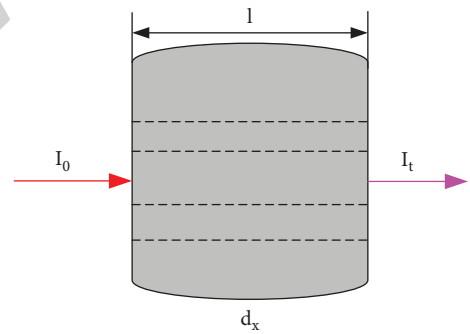

Figure 3: Propagation of light in a medium.

but also to the concentration or type of the liquid itself. To detect the transmission relationship of the liquid, (4) and (5) can be combined:

$$\alpha = \beta C \Rightarrow I_t = I_o e^{\beta C l}, \tag{4}$$

$$I_t = I_o e^{kT}. \tag{5}$$

From the above derivation, it can be found that different media would lead to different relationships between the intensity of incident light and outgoing light, and two factors cause the energy difference between the intensity of transmitted light and the intensity of incident light. These two factors are the distance transmitted and the medium transmitted, respectively. However, both are the same as changing the transmittance of light by changing the loss of light. Therefore, in the detection technology, as long as the

change law of light is used, the turbidity of liquid can be detected (that is, the value of the small particles in liquid). Next, two methods of liquid detection are introduced.

2.2.2. Scattering Turbidity Detection. The phenomenon of light scattering can be understood as the phenomenon that when a beam of light passes through a medium with inhomogeneous optical properties, light is observed in other directions than the incident light, that is, the phenomenon in which the direction of the incident light changes during the transmission process. Light scattering is very common in nature, and even in a beautiful landscape, as shown in Figure 4.

In scattering turbidity detection, scattering phenomena in nature are also used. In detection, a string of parallel lights is first input into the sample to be tested. At this time, the propagation of light would cause changes [23]. When the particulate matter in the solution is so small that it is smaller than the wavelength of the incident light, the scattered light intensity can be expressed as follows:

$$I_R = \mu \cdot \eta \cdot I_0, \tag{6}$$

$$\mu = \frac{K_R N V^2}{\lambda^4}, \tag{7}$$

$$\eta = \left(\frac{n_1^2 - n_2^2}{n_1^2 + 2n_2^2}\right)^2. \tag{8}$$

The scattered light intensity consists of three parts, namely, the incident light I_0, the refractive index η, and the refraction process μ. Among them, λ is the initial light wavelength; N and V are the particle number and volume of the liquid to be tested, respectively; K_R is the Rayleigh scattering coefficient, this coefficient is fixed in liquid detection. n_1, n_2 are the refractive indices of the particles.

In the detection process, since the liquid to be tested does not change frequently, it can be assumed that V and λ remain unchanged, then K_R is proportional to N. Formula (6) can be expressed as follows:

$$I_R = K' I_0 N, \tag{9}$$

$$K' = \frac{\mu}{N} \cdot \eta. \tag{10}$$

Among them, K' becomes a constant value, which can be used as a new refractive index.

When the particulate matter in the solution is larger than the wavelength of the incident light, the scattered light intensity can be expressed as follows:

$$I_M = K_M A N I_0. \tag{11}$$

The difference from Formula (9) is that when the particle diameter is larger, the refractive index changes. K_M is Mie scattering, which can better simulate the scattering characteristics of large particles, such as smoke and haze. A is the surface area of the particle. When the particles are larger, the concentration is larger and the scattered light intensity is larger, so that (11) can be simplified as follows:

$$I_S = K N I_0. \tag{12}$$

At this time, N is no longer the number of particles per unit volume but the concentration. K is the index of refraction after finishing.

2.2.3. Transmission Turbidity Detection. The process of light transmission is always accompanied by the process of absorption and loss of light energy. The traditional transmission turbidity detection method is also proposed by using the law of the energy attenuation change characteristics in the transmission process. The scattering-type detection is used to judge the intensity of the refracted light, while the transmission type is used to judge the transmitted light intensity, which focuses on the loss of light during the propagation process. Therefore, the intensity of light cannot be used as a criterion for evaluation during detection. What is used here is the energy of light. According to the glass duality of light, the photon energy collected after the incident light passes through the medium can be measured.

$$E = h\nu, \tag{13}$$

$$\nu = \frac{c}{\lambda}. \tag{14}$$

Formula (13) and (14) are basic formulae in optics, where h is Planck's constant. V is the frequency of light, which can also be obtained by dividing the speed of light c by the wavelength λ.

In a certain period of time Δt, the stable incident light transmission power used in the experiment can be expressed as follows:

$$P_t = \frac{(nM_t)h\nu/\lambda}{\eta \Delta t}, \tag{15}$$

Among them, M_t represents the photon pulse signal and η here represents the efficiency value of photon detection.

When using transmittance to detect liquid turbidity, there are two situations. When liquid is relatively pure, the transmission of light would hardly be hindered, which can be represented by a linear relationship. When turbidity is high, the transmission of light can only be expressed in exponential form. Specifically, it is necessary to set a threshold value to determine the turbidity of liquid. When turbidity is less than the threshold value, a linear relationship is used to express it so that the measurement can be performed quickly, and the lower limit of turbidity during detection is further improved. After referring to a large amount of literature, 0.1 NTU (turbidity unit) is used as the threshold. When the turbidity T is less than 0.1NTU, the calculation formula is (16); when the turbidity T is greater than 0.1 NTU, the calculation formula is (17).

Figure 4: Light scattering phenomenon.

$$M = K'' \cdot T + C_1, \tag{16}$$

$$M = K'' \cdot \sum_{n=0}^{\infty} \cdot \frac{T^n}{n!} + C. \tag{17}$$

Among them, K'' is the conversion coefficient, which can be obtained jointly by the transmission power and the law of refraction. Due to space constraints, the calculation is not detailed here. C, C_1 are constants.

2.3. Design and Construction of the Optical Fiber Detection System

2.3.1. Overall Design of the System. Based on the optical fiber single-photon detection technology, a system is designed for the transmission turbidity detection method and the scattering turbidity detection method introduced above, which makes the counting more convenient and the presented data more intuitive. To improve the measurement lower limit and stability of the detection system, the structure of the optical fiber probe is improved in this paper. Optical elements such as a new condenser lens and reflector are added to the probe port, which makes the entire optical fiber optical path structure more compact and stable and provides the possibility of finally realizing a wide dynamic measurement range and a portable structure. Figure 5 shows the overall structure of the system. The difference between the transmission type and the scattering-type detection methods is mainly present in the calculation method, and the difference in hardware is not very large. Therefore, the scattering-type turbidity detection system is described in detail. In Figure 5, with a fixed laser as the light source and a steady state laser emission, the power can be adjusted. The optical fiber attenuator can adjust the light intensity appropriately to achieve the effect of controlling the variable. The sample cell is used as the test storage location and is surrounded by metal material. The incoming direction of the fiber is adjusted by using the fiber collimator, which can ensure that the light beam can pass through the container accurately. Afterward, the measurement of the scattered light intensity and the photon energy is performed by the single-photon detection module. Finally, it is counted by using a photon counter, and the data results are further processed by using the computer and presented in a visual way. In terms of hardware selection, due to the high clock frequency of FPGA and a small internal delay, all control logic is completed by hardware, which is fast and efficient. Simultaneously, it has a very powerful hardware description language and simulation tools, which are convenient for checking the correctness of the results. The advantages of the field-programmable gate array (FPGA) in high-speed signal acquisition and processing are utilized, and the acquired pulse signals are processed on FPGA, which greatly improves the data processing efficiency.

The physical system is assembled based on the overall design architecture of the system and the desirability and cost-effectiveness of materials. The main hardware choices are shown in Table 1.

In the system test, the standard solution of formazin is used to detect turbidity. Formazin standard solution is often used in optical experiments because the formazin standard solution is stable and not easy to deteriorate, and it is also convenient to store. Additionally, the method for preparing the standard solution of formazin is relatively simple, and the materials are easy to obtain. In preparation, typically 25.0 ml of water is added to a 2.5 g urotropine sample to allow complete fusion, and then, 1.0 g of hydrazine sulfate is added to the urotropine aqueous solution. Finally, the mixture solution is diluted with water to 100 ml. After standing for a period of time, a standard formazin standard turbidity solution is prepared, and the turbidity of the solution is 400 NTU. It must be shaken well before use. In the experiment of this paper, the standard solution of formazin purchased from the laboratory was directly used for the test to avoid more errors in the experiment due to the errors caused by the preparation of the standard solution.

3. Turbidity Detection System Test Results

First, a multipoint measurement experiment with a wide turbidity range was carried out using the built-in measuring device. This paper was mainly carried out in three aspects: the preparation before the experiment, the result of the experiment, and the analysis of the result of the experiment. For the transmission detection technique, samples with 0–1000 NTU turbidity were tested herein and samples with 0–1 NTU turbidity were analyzed. For scattering detection,

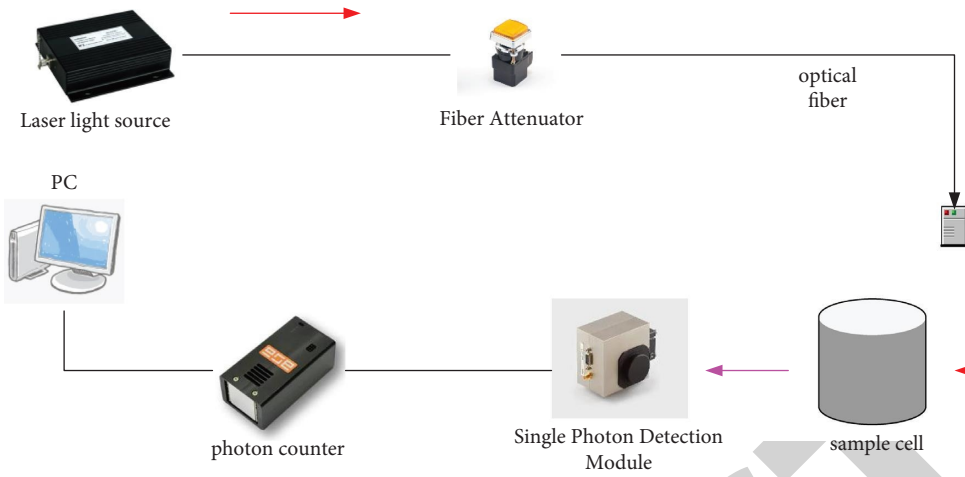

Figure 5: Schematic diagram of the fiber optic turbidity detection system.

Table 1: Hardware selection.

Serial number	Hardware	Product source
1	852 nm steady state laser	Thorlabs, DBR852S
2	Fiber attenuator	Thorlabs, VOA850-APC
3	Single-photon detector	PerkinElmer, SPCM-AQRH
4	Bandpass filter	Thorlabs, FB850-10

samples with a turbidity of 10–150 NTU were tested and compared with commercial Hach turbidity.

3.1. Test of the Transmission Fiber Inspection System. The designed transmission optical fiber detection system was tested. In the test, in order to highlight the advantages of the large detection range of the transmission turbidity detection system, samples of 0–1000 NTU were tested. In addition, in order to prove the effectiveness of the system, the light sources with multiple light intensities were also tested. The test results are shown in Figure 6.

In order to avoid adjusting the working state of the laser and obtain a wider dynamic measurement range as much as possible under a certain power, an optimal light intensity value should be sought for the system. Therefore, the influence of the variation of the light intensity of the light source on the measurement results of the system was discussed. In Figure 6, the abscissa represents the turbidity of the standard solution of formazin and the ordinate represents the photon count. Photon counting is adopted by the data acquisition module FPGA in the system. In order to reduce the error as much as possible, the photon counting period was particularly set to 1 ms, and the average value was used to represent the counting value of the system. From the data in Figure 6, there was an obvious exponential relationship between the photon count and the change in turbidity under different light intensities. The higher the turbidity, the lower the photon counts. When the turbidity

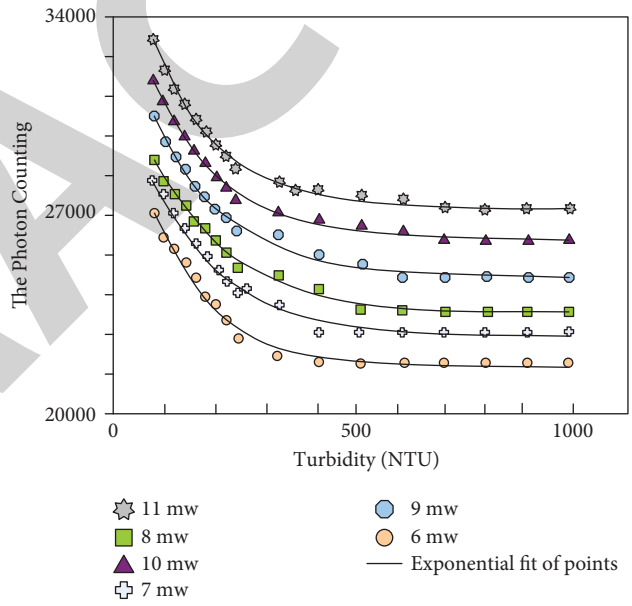

Figure 6: Measurement results under different light intensities.

reached 500 NTU, the photon counts did not change as the turbidity increased.

From the fitted curve, the system photon count values were on the curve, which indicated that the fitting was good. In Table 2, the fitting situation was calculated by using SPSS software. When the light intensity of the light source was 6–11 mw, the fitting indexes were 0.97, 0.97, 0.98, 0.98, 0.99, and 0.99, respectively. It can also be seen from the fitting index that the fitting index values were all greater than 0.8, and it can be considered that the fitting is excellent. This also proves that the transmission optical fiber turbidity measurement system designed in this paper has good performance for turbidity detection. However, it can also be found that with the increase of the light intensity in the light source, the fitting index also increased from 0.97 to 0.99, which shows that an appropriate increase in the light intensity can improve the testing effect of the system. The transmission

Table 2: Fitting degree of the transmission system under different light intensities.

Serial number	Incident light intensity (wm)	Fitted value
1	6	0.97
2	7	0.97
3	8	0.98
4	9	0.98
5	10	0.99
6	11	0.99

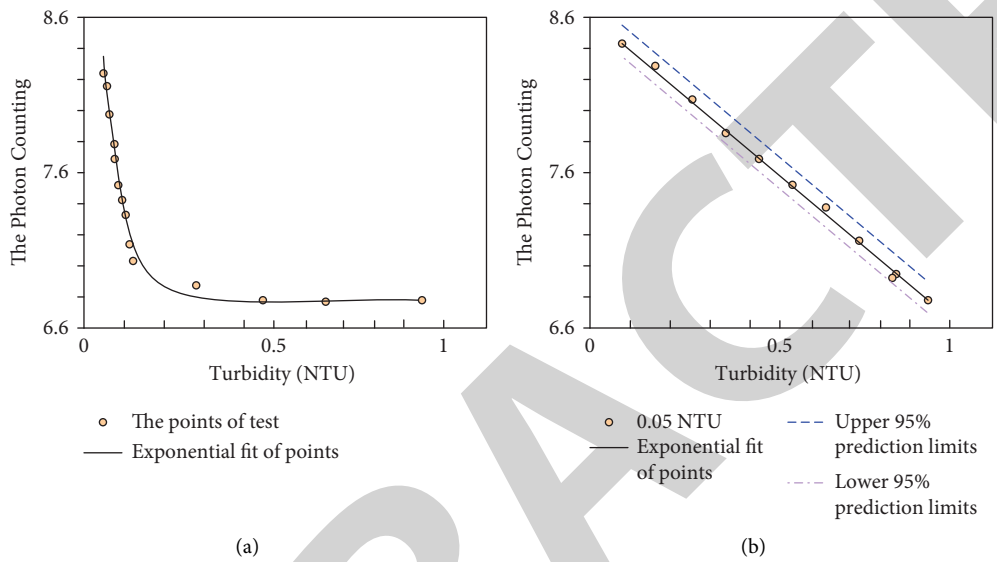

Figure 7: System results for low turbidity range measurements. (a) Low turbidity range measurement results. (b) Ultralow turbidity range measurement results.

detection system designed in this paper was not suitable for matching the strong light source. When the light source is very strong, the penetration of photons could damage parts of the instrument. Therefore, as far as the test results are concerned, when the light intensity was 11 mW, the detection effect of the system was the best.

In water quality testing, often low turbidity aqueous solutions need to be tested more. In a solution with low turbidity, it is almost transparent to the naked eye, and the number of particles in it would not affect the viewing of the naked eye. Therefore, it is of great significance for water quality detection to have a better detection effect on low turbidity solutions. In this regard, the transmissive system was further tested. The low turbidity range of 0-1 NTU and the ultralow turbidity range of 0–0.1 were tested, and the results are shown in Figure 7.

In Figure 7(a), at low concentrations, a similar trend to the large range is shown; both showed an exponential trend with a fit index of 0.98. In Figure 7(b), at ultralow concentrations, the light counts and turbidity showed a linear trend, and the fitting index was 0.99. Additionally, to reduce errors, multiple experiments were carried out for ultralow turbidity, and the upper and lower confidence intervals of the experimental data are also marked in Figure 7(b). It can be seen that the system tests showed two different trends at low turbidity, which was also consistent with the principle presented in the method of the introduction section. It was linear below the 0.1 NTU threshold and exponential above 0.1 NTU.

3.2. Test of the Scattering Fiber Detection System. In the sample cell, a clean glass bottle with good sealing performance was placed, and a small amount of formazin standard turbidity solution was added. In the experiment, 15 groups of samples with turbidity ranging from 10 NTU to 150 NTU were tested. Each turbidity sample was tested 5 times, and the average value represented the test value of the system. The result is shown in Figure 8.

In Figure 8, the abscissa represents the standard liquid turbidity and the ordinate represents the photon count. It can be seen that the photon counts of the scattering system showed a linear trend with the change in turbidity. The photon counts were distributed around the fitted line, and the values on both sides of the fitted line were the same. This showed that the photon count of scattered light in the 90° direction increased gradually with the increase of the turbidity value and was proportional to it. After calculation, the fitted value reached 0.99. This showed that in the system, as long as the photon count of scattered light in the 90° direction can be accurately measured, the solution turbidity can be reversed.

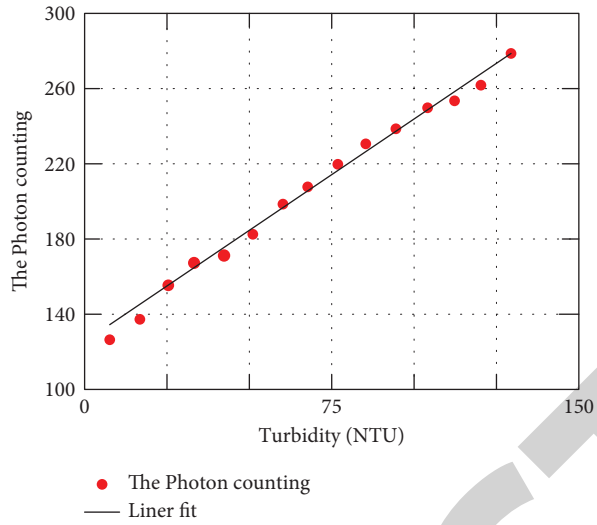

Figure 8: Scattered turbidity measurement results.

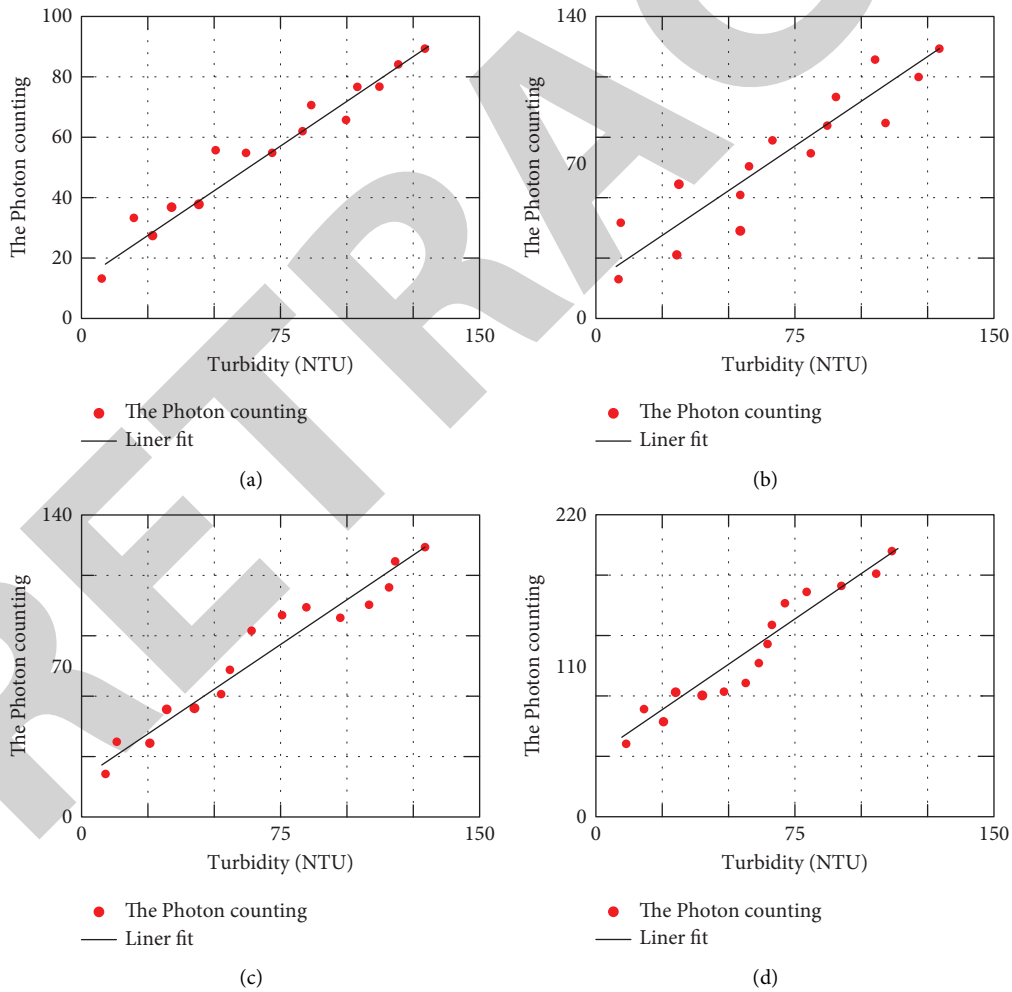

Figure 9: Influence of different incident light intensity values on the measurement results. (a) 1 wm. (b) 2 wm. (c) 3 wm. (d) 4 wm.

Scattering detection technology is more suitable for measuring medium and low turbidity because in the solution of high turbidity, the light would be scattered many times on the large particles, which greatly increases the error of the test. It is precisely the process of scattering that would affect the accuracy, so it is necessary to test the influence of the

Table 3: Fitting degree of the scattering system under different light intensities.

Serial number	Incident light intensity (wm)	Fitted value
1	1	0.94
2	2	0.96
3	3	0.98
4	4	0.99

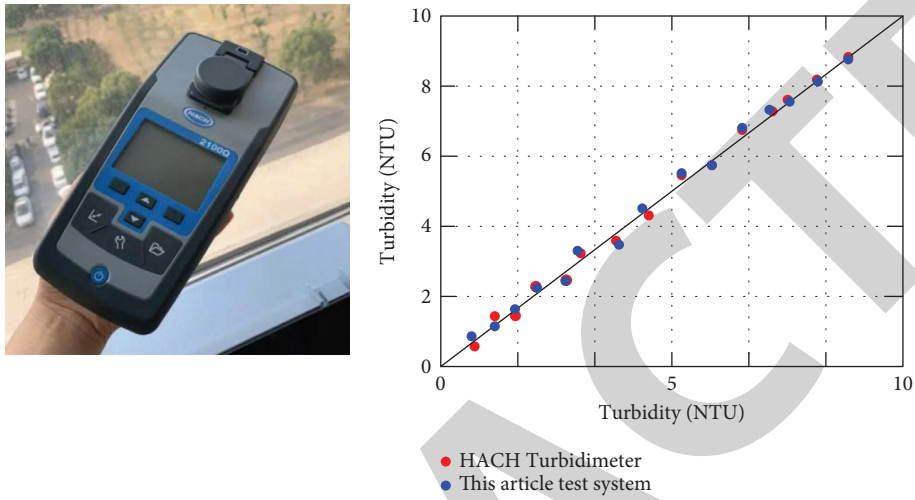

Figure 10: Comparison between the system in this paper and the turbidimeter. (a) HACH turbidimeter physical diagram. (b) HACH turbidimeter physical diagram.

light source intensity on the test accuracy. The test results are shown in Figure 9. Figures 9(a)–9(d), respectively, show the test results when the light intensity is 1 wm, 2 wm, 3 wm, and 4 wm.

By comparing the four groups of different incident light intensities as shown in Figure 9, it can be found that different incident light intensities would affect the degree of fitting between turbidity and photon counts. The fit values of the four groups of light intensities are shown in Table 3.

Table 3 shows that as the light intensity increased, the fitting degree also increased gradually. When the incident light was 4 wm, the fitting value was the highest, which was 0.99. This showed that the most suitable incident light intensity of the scattering turbidity detection system in this paper was 4 wm.

In order to further prove the accuracy of the system in this paper, the system in this paper was compared with more mature commercial turbidimeters in the experiment. The Hach 2100 Q turbidimeter was chosen for this article because of its wide measurement range and high accuracy. The comparison with the system in this paper can further illustrate the effectiveness of the system in this paper. In the experiment, the sample solution of 0–10 NTU was tested in this paper, and the test results are shown in Figure 10.

Figure 10(a) shows the actual picture of the commercial turbidimeter used in this paper, and Figure 10(b) shows a comparison result graph. In Figure 10(b), the blue dots are the test results of the scattering system in this paper, the red dots are the test results of the HACH turbidimeter, and the black solid line is the diagonal line, which represents the standard test result. The abscissa represents the true turbidity of the formazin standard solution, and the ordinate represents the detected turbidity. It can be seen from Figure 10(b) that the test results of the system in this paper had a high similarity with the test results of the HACH turbidimeter; the overall difference was not more than 2%, and both were near the diagonal. This also showed that the performance of the system in this paper was comparable to that of the more commonly used commercial turbidimeters in the market.

4. Conclusions

In this paper, a turbidity detection system was designed in detail, and the numerical simulation and parameter inspection of water quality particle detection were analyzed. To obtain a large-scale turbidity detection effect, a transmission fiber turbidity detection system based on single-photon technology was designed. The result was that the detection effect could be higher in the range of 0–1000 NTU. To test the accuracy, this paper also designed a scattering optical fiber turbidity detection system, which had a high detection accuracy at low and medium concentrations. After experimental verification, the system designed in this paper was similar to the results of the current commercial HACH turbidimeter, which showed that the system designed in this paper was more effective in turbidity detection. However, there are some flaws in this paper that deserve to be

improved. For example, data analysis and visualization modules can be integrated into the system so that the results of water quality testing can be displayed on the system interface intuitively. Therefore, in the follow-up research, the visualization of the data would be improved to design a more user-friendly detection system.

Data Availability

Data sharing is not applicable to this article as no datasets were generated or analyzed during the current study.

Conflicts of Interest

The authors declare that they have no conflicts of interest regarding the publication of this work.

Acknowledgments

This work was supported by (1) the General Project of Natural Science funded by the Education Department of Anhui Province (KJ2019JD13), (2) the Key Project of Natural Science funded by the Education Department of Anhui Province (KJ2019ZD56), and (3) the Project of Visiting Scholar funded by the China Scholarship Council (CSCNO.201908340023) and KTH.

References

[1] J. Passig, J. Schade, R. Irsig, L. Li, and R. Zimmermann, "Detection of ship plumes from residual fuel operation in emission control areas using single-particle mass spectrometry," *Atmospheric Measurement Techniques*, vol. 14, no. 6, pp. 4171–4185, 2021.

[2] H. Jia and X. L. Feng, "Very high-frequency silicon carbide microdisk resonators with multimode responses in water for particle sensing," *Journal of Microelectromechanical Systems*, vol. 28, no. 6, pp. 941–953, 2019.

[3] M. D. Graham, J. Cook, J. Graydon et al., "High-resolution imaging particle analysis of freshwater cyanobacterial blooms: flowcam analysis of cyanobacteria," *Limnology and Oceanography: Methods*, vol. 16, no. 10, pp. 669–679, 2018.

[4] R. Sultana, M. Hasan, M. R. Uddin, S. Ahmed, and A. Nahar, "Rainwater quality parameters at khulna city of Bangladesh," *International Journal of Environmental Health Research*, vol. 8, no. 2, pp. 49–54, 2020.

[5] C. Asbach, A. Schmitz, F. Schmidt, C. Monz, and A. M. Todea, "Intercomparison of a personal CPC and different conventional CPCs," *Aerosol and Air Quality Research*, vol. 17, no. 5, pp. 1132–1141, 2017.

[6] D. L. Huffaker, "InGaAs-GaAs nanowire avalanche photodiodes toward single-photon detection in free-running mode," *Nano Letters*, vol. 19, no. 1, pp. 582–590, 2019.

[7] S. Deng, A. P. Morrison, H. Liu et al., "High dynamic range photo-detection module using on-chip dual avalanche photodiodes," *IEEE Photonics Technology Letters*, vol. 31, no. 24, pp. 1940–1943, 2019.

[8] X. Zhou, X. Tan, Y. Lv et al., "Single-photon-counting performance of 4H-SiC avalanche photodiodes with a wide-range incident flux," *IEEE Photonics Technology Letters*, vol. 32, no. 14, pp. 847–850, 2020.

[9] M. Silver, P. Manurkar, Y. P. Huang et al., "Spectrally multiplexed upconversion detection with C-band pump and signal wavelengths," *IEEE Photonics Technology Letters*, vol. 29, no. 13, pp. 1097–1100, 2017.

[10] X. Ren, B. Xu, Q. Fei et al., "Single-photon counting laser ranging with optical frequency combs," *IEEE Photonics Technology Letters*, vol. 33, no. 1, pp. 27–30, 2021.

[11] B. Liu, Y. Yu, and S. Jiang, "Review of advances in LiDAR detection and 3D imaging," *Guangdian Gongcheng/Opto-Electronic Engineering*, vol. 46, no. 7, pp. 2019–2065, 2019.

[12] S. Saha, Y. Lu, S. Weyers, M. Sawan, and F. Lesage, "Compact fast optode-based probe for single-photon counting applications," *IEEE Photonics Technology Letters*, vol. 30, no. 17, pp. 1515–1518, 2018.

[13] Z. Wang, X. He, H. Shen, S. Fan, and Y. Zeng, "Multi-source information fusion to identify water supply pipe leakage based on SVM and VMD," *Information Processing and Management*, vol. 59, no. 2, Article ID 102819, 2022.

[14] K. S. Parmar, S. J. S. Makkhan, and S. Kaushal, "Neuro-fuzzy-wavelet hybrid approach to estimate the future trends of river water quality," *Neural Computing and Applications*, vol. 31, no. 12, pp. 8463–8473, 2019.

[15] G. Mandlburger, "Evaluation of single photon and waveform LiDAR," *Archives of Photogrammetry, Cartography and Remote Sensing*, vol. 31, no. 1, pp. 13–20, 2019.

[16] H. Terai, "4-2 Development of superconducting nanowire single-photon detector," *Journal of the National Institute of Information and Communications Technology*, vol. 64, no. 1, pp. 57–63, 2017.

[17] D. Shin, A. Kirmani, V. K. Goyal, and J. H. Shapiro, "Photon-efficient computational 3-D and reflectivity imaging with single-photon detectors," *IEEE Transactions on Computational Imaging*, vol. 1, no. 2, pp. 112–125, 2015.

[18] L. Yan, M. A. Raihan Miah, Y. H. Liu, and Y. H. Lo, "Single photon detector with a mesoscopic cycling excitation design of dual gain sections and a transport barrier," *Optics Letters*, vol. 44, no. 7, pp. 1746–1749, 2019.

[19] E. Iman and J. W. Zadeh, "Single-photon detectors combining high efficiency, high detection rates, and ultra-high timing resolution," *APL Photonics*, vol. 2, no. 11, Article ID 111301, 2017.

[20] S. Abba, R. Abdulkadir, S. Sh. Sammen et al., "Integrating feature extraction approaches with hybrid emotional neural networks for water quality index modeling," *Applied Soft Computing*, vol. 114, Article ID 108036, 2022.

[21] F. Gao, A. Khelif, S. Benchabane, and A. Bermak, "Shear horizontal phononic metasurface for in-liquid gravimetric biosensing," *IEEE Electron Device Letters*, vol. 42, no. 6, pp. 915–918, 2021.

[22] E. Botzung-Appert, V. Monnier, T. H. Duong, R. Pansu, and A. Ibanez, "Polyaromatic luminescent nanocrystals for chemical and biological sensors," *Chemistry of Materials*, vol. 16, no. 9, pp. 1609–1611, 2004.

[23] W. Fister, N. Goldman, M. Mayer, M. Suter, and N. J. Kuhn, "Testing of photogrammetry for differentiation of soil organic carbon and biochar in sandy substrates," *Geographica Helvetica*, vol. 74, no. 1, pp. 81–91, 2019.